Chitosan nanoparticles generation using CO2 assisted processes

Nibal Hijazi, Élisabeth Rodier, Jean-jacques Letourneau, Haithem Louati, Martial Sauceau, Nicolas Le Moigne, Jean-Charles Bénézet, Jacques Fages

Chitosan nanoparticles generation using CO_2 assisted processes

Nibal Hijazi [a,b], Elisabeth Rodier [a], Jean-Jacques Letourneau [a], Haithem Louati [a], Martial Sauceau [a], Nicolas Le Moigne [b], Jean-Charles Benezet [b], Jacques Fages [a,*]

[a] Université de Toulouse; École des Mines d'Albi; UMR CNRS 5302; RAPSODEE Research Centre, F-81013 Albi, France
[b] École des Mines d'Alès, Centre des Matériaux des Mines d'Alès (C2MA), 6 avenue de Clavières, F-30319 Alès, France

The current concerns of sustainable development make the biobased polymers the object of many studies. Chitosan is a biobased, biocompatible and biodegradable polysaccharide with antibacterial and cytocompatible properties. In this study, we aimed to generate chitosan particles with two processes using CO_2 under pressure, in order to decrease the use of organic solvent and to obtain nanoparticles.

The first is a supercritical anti-solvent process: CO_2 acts as an anti-solvent toward an acetic acid aqueous solution of dissolved chitosan in which ethanol was added to enhance the anti-solvent effect. The reciprocal miscibility of CO_2 with the solvents induces the reduction of their solvating power, leading to supersaturation at the capillary outlet and causing the crystallization of the particles.

This process led to the generation of more or less agglomerated chitosan nanoparticles with an individual average size of 378 nm.

In the second process, the pressurized CO_2 is dissolved in water to lower the pH. This in turn allows the chitosan to be dissolved and the resulting solution is sprayed, thanks to the pressurized CO_2, into a hot air stream. This new process allowed the generation of dried chitosan nanoparticles with a median size of 390 nm.

1. Introduction

Nowadays, mankind has to cope with global challenges in its attempt to protect the environment in the long term. For this purpose, sustainable industrial development has been encouraged. In the case of engineering of polymeric materials, sustainability issues impact the choice of raw materials, the design of material process, the consideration of life cycle assessment.

Among the studies carried out to date, an approach is to use biobased polymer materials and structure them at micro/nanometric scales to enhance some of their specific properties in order to create an original material with specific functional properties.

Several approaches have been proposed to develop biobased polymer nanocomposites, as the dispersion of inorganic particles such as clays in a polymer matrix [1]. An original approach is the synthesis of biobased polymer nanoparticles that could be used for further development of nanostructured biobased polymer assemblies. For this purpose, our study focused on the generation of polysaccharide particles. Polysaccharides represent a vast category of biobased polymers with specific functionalities, presently used in all sectors of human activities like materials science, nutrition, health care and energy and with large applications in industry. Within this family, chitosan, an amino-polysaccharide derived from chitin by deacetylation (deacetylation degree of at least 50%) which is the second most biosynthesized polymer after cellulose obtained mainly from crustaceans exoskeleton [2], was chosen to be the material for nanoparticle elaboration.

Chitosan is not only readily available but also biocompatible and biodegradable due to its two chemical functionalities, mucoadhesive with antibacterial and cytocompatible activities [3–5]. It is principally used in agriculture, water treatment, cosmetics, pharmaceutics and biomedical, food packaging [6].

Dash et al. [7] have recently reviewed the studies which have been conducted to generate chitosan particles from acetic acid aqueous solution to be used as carriers for drug delivery [7]: by spray-drying (2–10 μm [8]), emulsion-crosslinking (350–690 μm [9]), coacervation–precipitation (100–250 nm [10])... These processes are commonly used but have several drawbacks as the use of toxic solvents, surfactants and crosslinking agents implying their

Abbreviations: Ac Ac, acetic acid; Chit, chitosan; DSC, differential scanning calorimetry; EtOH, ethanol; SAS, supercritical antisolvent; SCASA, supercritical CO_2 assisted solubilization and atomization; sc-CO_2, supercritical carbon dioxide; TGA, thermogravimetric analysis; XRD, X-ray diffraction.

* Corresponding author. Tel.: +33 563 493 141; fax: +33 563 493 025.
E-mail address: Jacques.Fages@mines-albi.fr (J. Fages).

Nomenclature

C (kg m^3) solution concentration
DA (%) degree of acetylation
K (m^3 kg^{-1}), a constants of polymer/solvent system
K' Huggins constant
M_v (kDa) viscosity average molecular weight
η (mPa s) polymer solution dynamic viscosity
η_0 (mPa s) pure solvent dynamic viscosity
η_{int} (m^3 kg^{-1}) intrinsic viscosity
η_{rel} relative viscosity
η_{sp} specific viscosity
P_{Si} (MPa) pressure in the separator i
P_V (MPa) pressure in the vessel
pH_i pH of the chitosan solution before the experiment
pH_f pH of the chitosan solution after the experiment
Q_{chit} (mg s^{-1}) chitosan solution injection rate
Q_{CO2} (mg s^{-1}) CO_2 injection rate
T_V (K) temperature in the vessel
w_i (%) mass fraction of the component i

residual presence in the generated material, the use of high temperatures, the need of additional steps as purification and drying... In this context, particular attention has been paid to the use of supercritical carbon dioxide (sc-CO_2). Indeed, its ability to dissolve in large quantities in many polymers [11], enough to modify their properties (viscosity, surface tension...), may help to improve the composite materials produced while minimizing the use of harmful solvents that are usually difficult to recycle. In addition, the use of sc-CO_2 is well established for the elaboration of fine particles [12].

With the "Supercritical Assisted Atomization" process (SAA) [13], 1% acetic acid aqueous chitosan solution allowed the generation of particles ranging mostly between 0.1 and 1.5 μm. CO_2 was used as an expansion agent. Using a comparable process with an enhanced mixing device before depressurization, the "Supercritical fluid Assisted Atomization" introduced by "Hydrodynamic Cavitation Mixer" (SAA-HCM) [14], several molecular weights of chitosan were tested in order to evaluate their influence on the generated particles; particles with a diameter ranging between 0.2 and 5 μm were obtained from aqueous acidic solutions. Particle size distribution was strongly dependent on the molecular weight.

In this study, we investigate the generation of chitosan particles by two CO_2 based processes, Supercritical Anti-Solvent (SAS) and sc-CO_2 assisted solubilization and atomization (SCASA). CO_2 is expected to act as an anti-solvent in the first process and as a solubilization and expansion agent in the second process. The influence of processing conditions is studied for both techniques and the size distribution, crystallinity, degree of deacetylation and thermal stability of the generated particles are characterized.

2. Materials and methods

2.1. Materials and preliminary characterizations

Commercial chitosan extracted from shrimp shells was purchased from France Chitine (France). Purity is not given; possible impurities usually are residual chitin, inorganic compounds, proteins, chloride... [15]. Its viscosity, given by the supplier, is about 50 mPa s for a 1% (w/w) chitosan/acetic acid solution, measured by LVT Brookfield viscometer at 298 K. The acetylation degree DA, measured by the supplier using IR spectroscopy is around 10%. When chitosan is put into demineralized water, the pH of the resulting dispersion is around 13, which indicates the presence of residual NaOH in the commercial powder.

Table 1
Composition and viscosities of chitosan solutions used for the determination of chitosan M_v.

Mass composition (%)				Viscosity (mPa s)
Water	Acetic acid	Chitosan	m_{total} (g)	
90.90	9.10	0	22	1.2
89.89	8.99	1.12	22.25	31.3
88.89	8.89	2.22	22.5	114.3
87.91	8.79	3.30	22.75	258.6

Acetic acid (90%), sodium hydroxide and potassium hydroxide were purchased from Prolabo (France); ethanol (96%) was obtained from VWR (France). CO_2 (purity 99.995%) was supplied by Air Liquide (France) and used without any further purification.

The viscosity average molecular weight M_v of chitosan was estimated using Mark–Houwink Sakurada law:

$$[\eta_{int}] = K\, M_V^a \tag{1}$$

K and a were estimated to be respectively $4.74{\cdot}10^{-6}$ m^3 kg^{-1} and 0.72 [16].

Previously, the relative η_{rel} (Eq. (2)) and specific η_{sp} (Eq. (3)) viscosities were evaluated for several concentrations of chitosan solutions (Table 1) in order to deduce the value of the intrinsic viscosity $[\eta_{int}]$ of chitosan using Huggins relation (Eq. (4)):

$$\text{Relative viscosity} \quad \eta_{rel} = \frac{\eta}{\eta_0} \tag{2}$$

$$\text{Specific viscosity} \quad \eta_{sp} = \frac{\eta - \eta_0}{\eta_0} \tag{3}$$

$$\text{Huggins} \quad \frac{\eta_{sp}}{C} = K'[\eta_{int}]^2 \times C + [\eta_{int}] \tag{4}$$

The viscosity of chitosan solutions was determined using a rotational rheometer (RheoStress 600, Thermo Scientific, USA) using a 60 mm diameter plane–plane geometry, in continuous mode for shear rates between 0 and 500 s^{-1}.

In Huggins equation, $[\eta_{int}]$ is the intercept point of the line $(\eta_{sp}/C) = f(C)$ and its value was found to be about 0.13 m^3 kg^{-1}. Huggins equation is specifically applicable for very low concentrations with $[\eta_{int}]{\cdot}C \ll 1$ [17]. The extrapolation of this Eq. (4) above this limit induce a maximum value of $[\eta_{int}]{\cdot}C$ of 4.5 for the tested concentrations, which is considered as acceptable. Therefore, the molecular weight considered was calculated with Huggins equation and found to be 62 kDa.

2.2. Methods

2.2.1. Preparation of chitosan solutions

2.2.1.1. Chitosan solutions for SAS process. Chitosan solutions of different concentrations were prepared by dispersing chitosan powder into water, followed by addition under stirring of diluted acetic acid to dissolve chitosan. A 50/50 w/w ethanol/water (Sol3) solution was also prepared to enhance the anti-solvent effect of sc-CO_2 due to the very good miscibility of CO_2 and ethanol. The composition and some properties of the various solutions are presented in Table 2.

The surface tension and density were determined by an ILMS tensiometer (GBX instruments, France) using Wilhelmy plate method and the calibrated float method, respectively.

Afterwards, the solution is filtered under vacuum conditions through a nitrocellulose membrane with a cutting threshold value of 3 μm to remove the non-solubilized impurities. The amount of impurities retained on the membranes was about 6 mg and was neglected.

Table 2
Compositions of tested chitosan solutions during SAS process.

	w_{water} (%)	w_{EtOH} (%)	w_{AcAc} (%)	w_{Chit} (%)	m_{total} (g)	Surface tension[a] ($mN\,m^{-1}$)	Density[b] ($kg\,m^{-3}$)
Sol1	87.9	0	11.0	1.1	45.5	46.94	1.02
Sol2	87.0	0	10.8	2.2	46	–	–
Sol3	49.1	49.1	1.2	0.6	81.5	30.05	0.93

[a] Surface tension is given with $\pm$0.5 $mN\,m^{-1}$.
[b] Density is given with $\pm$0.001 $kg\,m^{-3}$.

Table 3
Compositions of the alkaline recovery solutions.

	w_{base} (%)	w_{water} (%)	m_{total} (g)
Recov1_NaOH	7.4	92.6	21.6
Recov2_KOH	2	98	51.0
Recov3_KOH	1	99	50.5

Table 4
Compositions of chitosan suspensions used for the SCASA process.

	w_{water} (%)	w_{Chit} (%)	m_{total} (g)
Susp1	99.50	0.50	502.50
Susp2	99.38	0.62	402.50
Susp3	99.37	0.63	503.14
Susp4	99.38	0.62	603.75

2.2.1.2. Alkaline recovery solutions for SAS process. Alkaline solutions of sodium and potassium hydroxide at various concentrations were prepared (Table 3) for the solid generation and the recovery of chitosan particles.

2.2.1.3. Chitosan dispersions for SCASA process. As commercial chitosan contains residual sodium hydroxide, it was previously washed with water to lower the initial pH of aqueous dispersions. It was then filtered and oven-dried. The pH was thus lowered to 8.

Chitosan suspensions with varying concentrations and volumes were tested using this process (Table 4). Total quantity or volume treated in an experiment was varied in order to observe its impact on the process yield.

2.2.2. Experimental set-up

2.2.2.1. SAS process. The experiments were carried out using a versatile pilot plant (Separex, France). A scheme of the apparatus is given in Fig. 1.

Liquid CO_2 is pumped up to a supercritical pressure by a diaphragm pump P1 (Lewa, Germany). Compressed CO_2 goes through a heat exchanger (E2) previously set at 313 K in order to reach the critical conditions of the CO_2, before entering into the 1.2 dm^3 vessel V (Parr Instrument, USA).

The vessel (V) has multiple sapphire windows, a magnetic stirrer with a maximum torque of 1.8 N.m and a removable heating collar. The pressure in the autoclave is controlled by a back-pressure regulator (D). A particulate filter (F) is placed at the exit of the vessel to prevent the particles from contaminating the rest of the circuit. Three cyclonic separators (S1, S2 and S3) are used to separate the solvents from CO_2 by gradual depressurization, the pressure being set by micrometer valves. An active carbon packed bed (AC) is placed after the separators to purify the CO_2 before cooling by (E1) and returning to storage (T). HPLC pump (P2) (Gilson, USA) allows the introduction of the chitosan solution in the vessel (V) through a stainless steel capillary tube (O) whose length is 10 mm and inner-diameter is 100 μm.

2.2.2.2. SCASA process. Fig. 2 displays the schematic diagram of the SCASA apparatus.

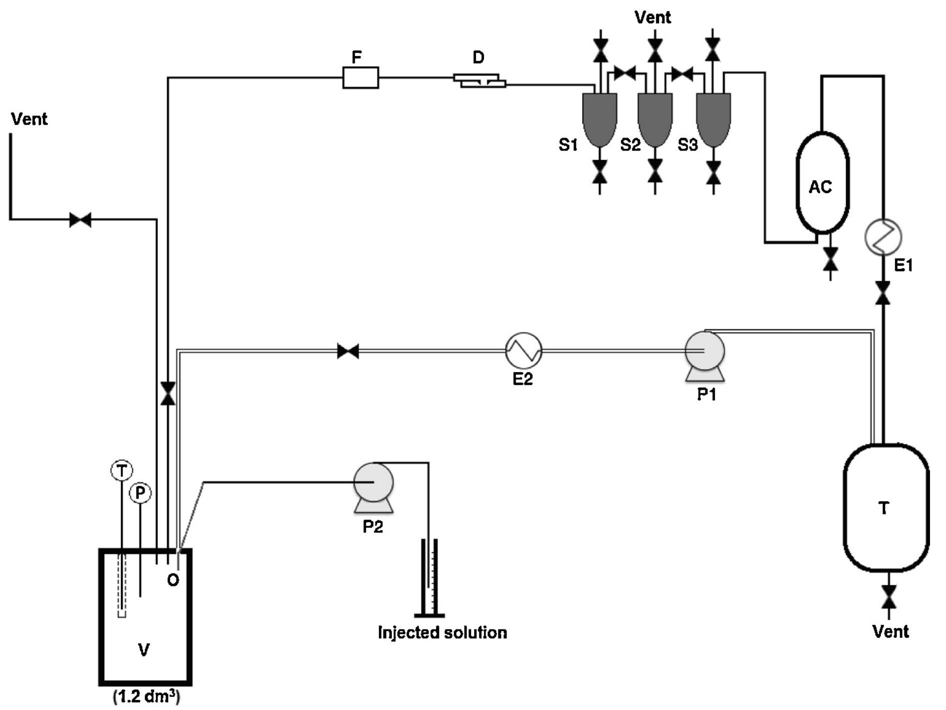

Fig. 1. Schematic representation of the SAS apparatus.

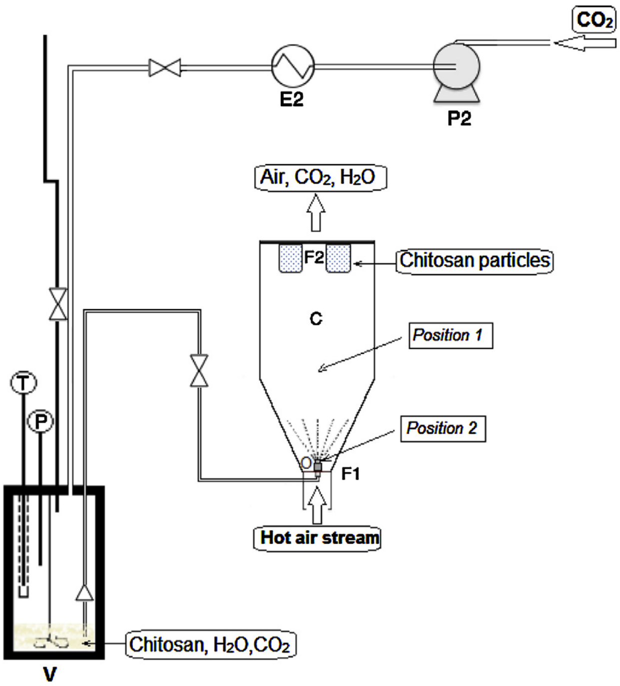

Fig. 2. Schematic representation of the SCASA apparatus.

The introduction of CO_2 into the pilot plant and the vessel (V) are similar to the SAS process apparatus. The vessel V is used to prepare the chitosan solution. A spraying orifice (O), the stainless steel capillary tube already used in SAS process or a nozzle, is placed at the exit of the vessel (V) and fixed at the inlet of a fluidized bed C (Aeromatic-Fielder, Switzerland), which acts as an atomizing device. The fluidized bed is flowed by hot air with adjustable velocity and temperature in order to dry the generated particles during spraying. Two filtering devices (F1 and F2) are placed at both ends of the fluidized bed. F1, a stainless steel wire screen allows a homogeneous distribution of entering hot air. F2, equipped with four filter bags and stainless steel wire gauze on top of them, allows retaining particles.

2.2.3. *Chitosan particles generation*

2.2.3.1. SAS process. An alkaline solution is placed inside the vessel (V) to receive and stop further evolution of the generated particles by neutralizing any residual acidity remaining on the particles and induced by CO_2. At first, only sc-CO_2 is introduced in the vessel (V) and circulated in order to stabilize pressure, temperature and flow in the system before injecting the chitosan solution. Pressures are adjusted by the back-pressure regulator and the micrometric valves. Once a steady state is reached, the chitosan solution is injected through the capillary tube into the sc-CO_2 flow at 1 ml min^{-1} (or 16.7 mm^3 s^{-1}). The reciprocal miscibility of CO_2 with acetic acid and ethanol of the chitosan solution induces an anti-solvent effect allowing the particle crystallization at the exit of the capillary. CO_2 loaded with solvents flows out toward the separators, from which the liquid phase at the bottom are purged frequently to recover solvents. At the end of the injection, the vessel is depressurized and the particles in suspension are collected.

To eliminate the salts formed by the reactions between CO_2, alkaline solutions and acetic acid such as sodium/potassium carbonate and sodium/potassium acetate, the suspensions are washed with distilled water ($6 < pH < 7$) and filtered under vacuum using a polypropylene membrane cutting at 0.45 μm. The operation is repeated several times before freeze-drying (Freeze-dryer Christ Alpha 1-4 LDC-1 M, Germany) and performed at 3 kPa with a freezing temperature of 261 K.

2.2.3.2. SCASA process. The key-point of this process is to replace diluted acetic acid by water acidified by pressurized CO_2: chitosan powder is first dispersed in distilled water and placed inside the vessel (V) under stirring. The vessel is then filled and pressurized with CO_2. Under high pressure (20 ± 0.5 MPa) and at moderate temperature (298 ± 2 K), the acidifying power of the CO_2 causes the dissolution of the chitosan powder. Pressure and temperature are chosen so as to favor dissolution of CO_2 into water. Calculations are based on the work of Diamond and Akinfiev [18] showing that the value of the CO_2 mole fraction in water is 2.6 % (mol/mol) at 20 MPa and 308 K. The pH of the CO_2-acidified water was calculated according to Peng et al. [19]: at 308 K and 20 MPa, pH is 2.95 and at 383 K and 20 MPa, pH is 3.26. These authors proposed a model whose results were compared to the measurements performed by Read [20]; both result sets were found to be consistent.

In such conditions, 48 h of stirring allows the dissolution of the tested amount of chitosan. The result is an instable emulsion of two phases: a heavy phase of CO_2-saturated aqueous chitosan solution and a light phase of water-saturated sc-CO_2. It is then pushed toward the capillary (inner diameter 100 μm) or the spraying nozzle (outlet diameter 340 μm) by an upstream-pressurized CO_2 flow rate. This flow consists of heated CO_2 (at 333 K) introduced in the vessel (V) continuously to maintain pressure at 14 ± 1 MPa. It is then sprayed at the bottom of the fluidized bed (C) and carried upward by the flowing air stream, which is at atmospheric pressure, previously heated up to 368 ± 5 K and injected with a flow rate of 2 m^3 min^{-1}. During the depressurization, CO_2 turns back to its gaseous state leading to a supersaturation and an atomization of chitosan-loaded droplets; the hot air stream simultaneously eliminates liquid water. The flow of preheated CO_2 allows the preheating of the sprayed solution for a better drying. The airflow velocity is kept at its highest level and unchanged during the process to avoid the sprayed solution from sticking to the fluidized bed walls, while the stirring rate in the vessel (V) is adjusted to keep a visually homogeneous emulsion and to keep a constant temperature of the outlet flow leaving the fluidized bed (C). After spraying, particles are collected in the filters (F2). After the experiments, the pH of the residual solution inside the vessel was found to be around 5 after depressurization, which indicates that water was indeed acidified by the pressurized CO_2.

2.2.4. *Commercial and generated chitosan particles characterization*

Particle size distribution and mean particle diameter in the suspensions were measured using a Nano Zetasizer (Malvern Instruments, France) by the evaluation of the Brownian diffusion coefficient (for SAS process) or a Mastersizer 2000HS (Malvern Instruments, France) by light diffraction pattern using ethanol as dispersing agent (for SCASA process).

Dry chitosan particles were visualized with an Environmental Scanning Electron Microscope (ESEM XL30 FEG, FEI Philips, Netherlands). For each sample, over 500 particles from at least four pictures were analyzed with a numerical caliper integrated in the image acquisition software in order to determine mean particle diameter and the particle size distribution weighted in number.

Crystal structures of commercial and generated particles were investigated by X-ray diffraction (XRD) using an AXS D8 Advance Brüker diffractometer (Germany) equipped with a Cu cathode ($\lambda = 1.54$ Å). Measurements were performed in the range $2\theta = 5–60°$ under 40 kV and 40 mA with a step size of 0.007°.

Acetylation degree of chitosan was estimated by FTIR using a Brüker IFS 66 spectrophotometer (Brüker Optics, Switzerland). FT-IR spectra were recorded in attenuated total reflectance (ATR) mode

Table 5
Processing parameters of the various experiments performed using the SAS process.

Test	Chitosan solution used	pH	Processing parameters					Recovery solutions	
			Q_{chit} (mg s^{-1})	Q_{CO2} (mg s^{-1})	[a]P_{S1} (MPa)	P_{S2} (MPa)	P_{S3} (MPa)	pH_i	pH_f
M0	Sol1		14.8	–	–	–	–	–	2.4
M1	Sol3	4.9	14.0	1500	7.2	6.9	4.2	–	4.6
M2	Sol2	3.4	14.8	1150	11.3	10.4	5.4	12.3	6.9
M3	Sol3	4.9	14.7	1650	7.1	6.6	4.0	13.5	7.9
M4	Sol3	4.9	14.8	1450	7.1	6.6	4.0	13.3	6.3

[a] P_{S1}, P_{S2} and P_{S3} are given with an absolute accuracy of ±0.5 MPa.

in the range 4000–400 cm^{-1} with a resolution of 4 cm^{-1} and 32 scans, for 3–5 mg of chitosan powder.

Several correlations have been proposed in the literature to calculate the acetylation degree based on the changing of the chemical structure of the material observed on the FT-IR spectra [21]. Several have been tested; the chosen correlation below is the one that gave the most reproducible values of DA.

$$DA = 31.92 \times \left(\frac{A_{1320}}{A_{1420}}\right) - 12.20 \tag{5}$$

where A_{1320} and A_{1420} are respectively the absorbance of the peak at 1320 cm^{-1} related to the acetylated amine function and the peak at 1420 cm^{-1} related to the —C—H bending. This last one revealed to remain almost unchanged for different known acetylation degrees and was then used as the reference peak.

A differential scanning calorimeter (TGA-DSC 111 Setaram, France) was used to characterize the thermal stability of the commercial and generated chitosan particles (5–20 mg). Thermograms were obtained between 298 and 1073 K with a heating rate of 10 K min^{-1} in a nitrogen gas stream of 50 cm^3 min^{-1}.

3. Results and discussion

3.1. Particles generation using SAS process

Two main series of tests were performed: the first (M0 and M1) aimed to test the influence of ethanol used in the chitosan solution; the second (M2–M4) was meant to study the impact of the recovery solution used to collect the particles previously formed and to keep them in suspension. Recovery solutions 1, 2 and 3 (see Table 3) were used respectively in tests M2, M3 and M4. All the experiments were made at T_V = 308 K ± 2 K and P_V = 17.6 ± 0.3 MPa. The conditions of the different experiments are shown in Table 5.

In the absence of recovery solution, the effect of ethanol on the particle generation was evaluated. The experiments showed that either in the presence or the absence of ethanol (M1 and M0 tests respectively), no particles were observed in the vessel at the end of the experiment. However, adding ethanol, which is highly miscible with CO_2 at high pressure, lowers the solution surface tension and facilitated the reciprocal transfer of solvents into the sc-CO_2. This was easily visualized through the volumetric expansion of the solution droplets (not shown in this paper). This usually promotes the particle generation by SAS and a better removal of acetic acid. Furthermore, the pH of the solution collected in the vessel after these tests was measured. In the absence of ethanol, the pH was found to be about 2.4 ± 0.2 while it was of 4.4 ± 0.2 in the presence of ethanol. In both cases, the pH was far lower than the pK_a of chitosan (≈6.3) [2]. This acidity may come from: (1) the presence of residual acetic acid in the vessel that may not be driven out by the sc-CO_2; (2) the presence of carbonic acid H_2CO_3 due to the solubility of CO_2 in water under pressure. As previously mentioned, the value of mole fraction of CO_2 in water is 2.6% (mol/mol) at 20 MPa and 308 K. This should induce a pH of 2.95 in the solution. The pH being higher in the presence of ethanol and close to 4 confirmed the better removal of acetic acid and the improvement of the anti-solvent effect. However the medium was still too acidic to prevent the redissolution of previously formed chitosan particles. This should explain their absence in the solution.

It was also found that when the recovery solution contained only demineralized water (not presented in this paper), the results were similar to the experiments without recovery solution. Therefore, a recovery solution was added to neutralize the acid excess (tests M2–M4). Two kinds of alkaline solutions were placed separately in the vessel to be tested as a medium to collect particles: sodium hydroxide solutions (M2) and potassium hydroxide solutions (M3 and M4). For all the tested alkaline solutions, suspended particles were observed at the end of the experiment and the pH was equal or higher than 6.3. Nevertheless, after freeze-drying, the SEM observation showed the presence of crystal layer on the particles surface (Fig. 3).

The nature of these crystals was determined by XRD analysis. It was found that sodium acetate and carbonate crystals are formed by precipitation reactions that occurred by contact of the alkaline solutions with CO_2 and acetic acid. Hence, washing the suspensions before freeze-drying was necessary. Potassium hydroxide based solutions were found to be more suitable regarding the lower amount of formed crystals, which ease the washing.

M3 and M4 tests differed in the concentration of potassium hydroxide. The results of these two tests are shown in the SEM images (Fig. 4) and compared to commercial chitosan particles (Fig. 4a). For M3 (Fig. 4b), nanoscaled particles (the average diameter measured by Nano Zetasizer is 378 ± 13 nm) were observed in a porous network of chitosan. M4 produced better defined nanoparticles (Fig. 4c) with an average diameter of 820 ± 19 nm. In both

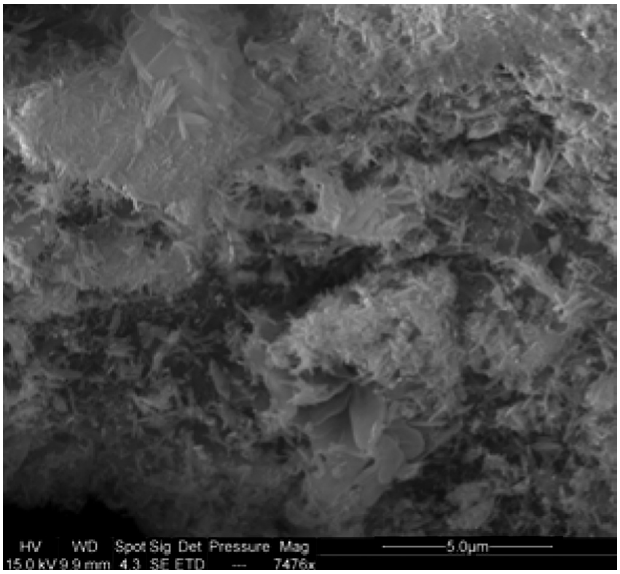

Fig. 3. ESEM observation of freeze-dried particles obtained from the M2 test.

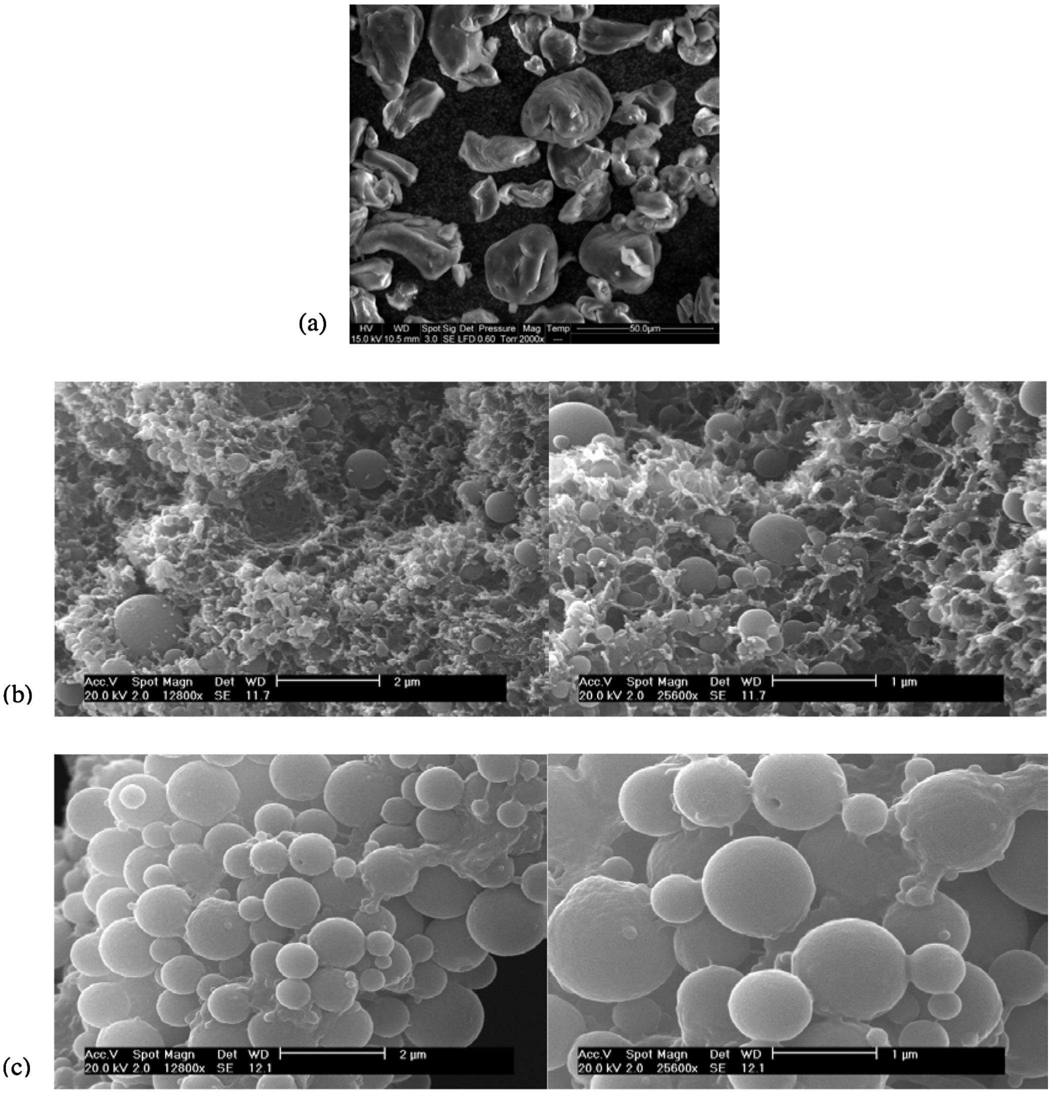

Fig. 4. SEM photographs of commercial chitosan (a) and particles generated by the SAS process; M3 test: chitosan nanoparticles fixed in a porous chitosan network (b) and M4 test: well defined chitosan nanoparticles (c).

cases, the average diameter of the generated particles was submicronic, which confirms the ability of the SAS process to generate nanoparticles of chitosan.

However, these two different generated morphologies, i.e. nanoparticles embedded in a porous chitosan network and well defined chitosan nanoparticles, could be explained by the coexistence of two main generation phenomena: (1) particle generation by anti-solvent effect of the sc-CO_2 at the exit of the capillary (Fig. 5a) and (2) porous network generation (Fig. 5b) which is firstly due to the pH transition (that induces a phase separation [22] and particle coagulation occurring in basic media) once the injected chitosan is in contact with the alkaline solution and secondly to the CO_2 desorption. These two competing phenomena may vary significantly for even small pH variations; indeed, mainly the final pH of the recovery solution differs between M3 and M4 experiments. The strong influence of the chemistry of the systems involved, in particular the pH that gradually evolves during the dissolution and degassing of CO_2 and the washing phase, appeared to alter the organization of chitosan channels during phase separation.

Like SAA [13] and SAA-HCM [14] processes, SAS process led to chitosan nanoparticles from acetic acid solution with a large size distribution. However, the process used to obtain dry particles was different: the first two processes allowed the generation of dry particles by heating at high temperature in the presence of CO_2 as expansion agent. The SAS process allowed the generation of dispersed solid particles in the recovery solution which needs to be dried afterwards. The need for a post treatment and the lack of control of the physical and chemical parameters of the process may have induced lower reproducibility than in SAA process.

3.2. Particles generation using SCASA process

Different chitosan suspensions were tested using this process (Table 6). Furthermore, the influence of the nature of the spraying device and its location on the particle generation was evaluated.

The yield given in Table 6 is the ratio of the weight of chitosan particles and the weight of chitosan introduced in the vessel (V). Note that some solution remains in the bottom of the vessel at the end of the experiment (less than 20% of the introduced solution). Note also that the particle collecting device (F2) is not optimal yet and has to be enhanced; indeed finest nanometric particles may be lost in the vent. The yields given are therefore underestimated.

Table 6
Processing parameters of the various experiments done by SCASA process.

Test	Suspension	Spraying device			Solid generation yield (%)
		Type	Position	Diameter	
M'1	Susp1	Nozzle	2	Outlet: 340 μm	Not evaluated
M'2	Susp1	Capillary	1	Inner: 100 μm	21.4
M'3	Susp2	Capillary	2	Inner: 100 μm	25.5
M'4	Susp3	Capillary	2	Inner: 100 μm	22.4
M'5	Susp4	Capillary	2	Inner: 100 μm	33.4

The use of a nozzle (M'1 test) led to spraying flow rate too high compared to the drying airflow rate: a wet deposit of the sprayed solution was observed on the dryer wall. A dried film was then collected with very few particles on its surface (Fig. 6a). A capillary allowed to reduce significantly the spraying flow rate and two cases were considered regarding the location of the capillary. First, the capillary was placed in the middle of the air column (*position 1*) and oriented against the air stream (M'2) in order to have a longer trajectory and a better drying: a film deposit and particles of chitosan were both observed. The film deposit was on the dryer wall because the solution was sprayed too close to the bottom part of the column before the air stream could dry it. Chitosan particles were collected on the filters F2. As shown in Fig. 6b, these particles are spherical. Some of them are hollow-shaped, which could be explained by the desorption of the CO_2 during the solidification of chitosan spheres.

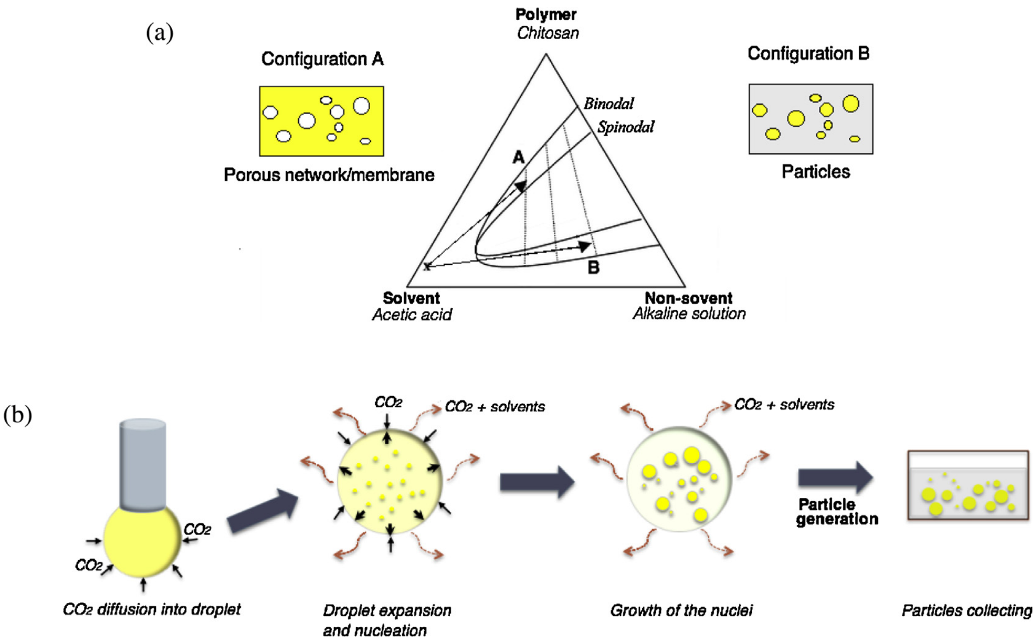

Fig. 5. Schematic representation of the mechanism of phase separation (a) and particle generation by anti-solvent effect (b) during the SAS process.

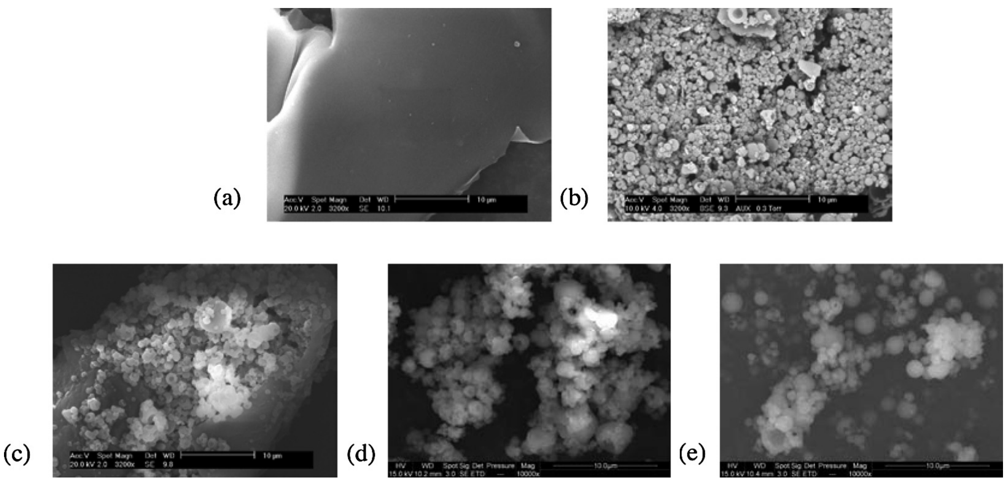

Fig. 6. SEM photographs of chitosan particles generated by the SCASA process: M'1 (a) M'2 (b), M'3 (c), M'4 (d) and M'5 (e) tests.

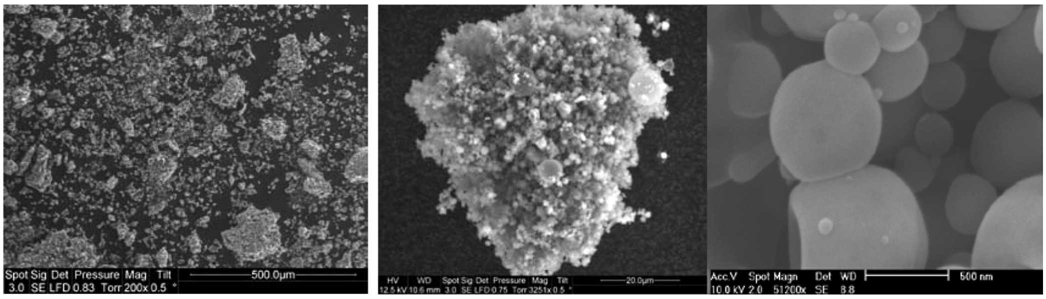

Fig. 7. Different scales of structures of chitosan generated particles by SCASA process.

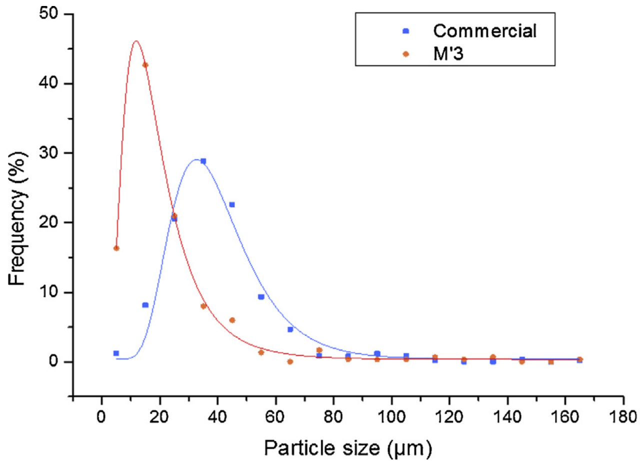

Fig. 8. Particle size distribution as determined from SEM pictures for commercial and generated chitosan by SCASA process. Dots refer to the measured values and the line refers to a lognormal law.

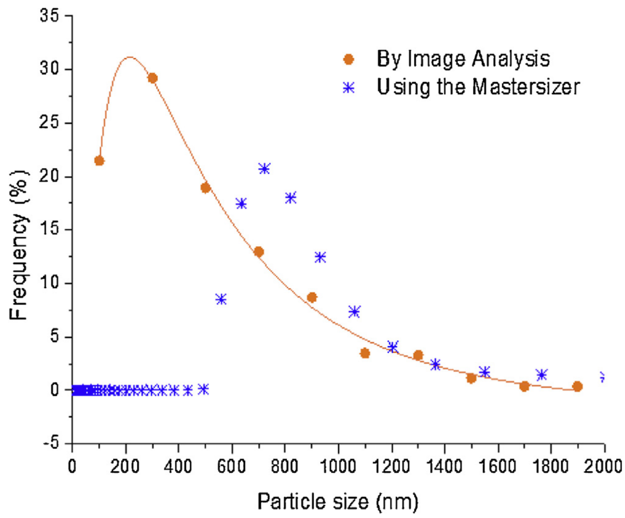

Fig. 9. Particles size distribution for generated chitosan by SCASA process (M'3 test). Dots refer to the measured values and the line refers to a lognormal law.

Then, when the capillary was placed upward at the bottom of the drying column (*position 2*) (M'3, M'4, M'5), the film deposit on the walls was negligible compared to the previous configuration and the particles yield of the process was enhanced. The variation of chitosan concentration from 0.5% to 0.62% (M'2 and M'3 tests, respectively) as well as the initial solution volume (M'3 to M'5) did not seem to significantly affect the particle generation nor the particle size (Fig. 6b–e). In all cases, particle size distribution is large as will be discussed below.

Generated particles have a bi-modal size distribution: nanoscaled particles for the most part and microscaled particles mainly due to the agglomeration of nanoparticles as shown in Fig. 7. The particle size distribution was determined by analyzing SEM pictures as follows: a first measurement was done at a micrometric scale corresponding to the lowest magnification of SEM pictures. The results are shown on Fig. 8. At this scale, for several experiments (not shown in this paper), the SCASA process reduced the size of the particles compared to the commercial chitosan powder.

A second measurement was done at the highest magnification of SEM pictures, where a large number of nanometric spherical particles was detected with a median size of 390 nm and less than 15% of the measured particles larger than 1 µm (Fig. 9).

Size was also evaluated by laser diffraction using a Mastersizer 2000HS: the number weighted size distribution is monomodal with a mean diameter of 721 nm. This diameter is higher than in Fig. 9 because of some remaining aggregates in the liquid dispersing medium but both measurement methods are consistent.

The particle size is hardly comparable to those obtained by Reverchon and Antonacci [13] and Shen et al. [14] since the used chitosan molecular weights and chitosan solution concentrations, parameters that highly impact the particle size according to Shen et al. [14], were different. The influence of processing parameters, chitosan properties and solution concentration on the particle size and the particle size distribution has not been explored deeply yet. Nevertheless, SCASA process generates repeatedly chitosan nanoparticles. Furthermore, compared to processes using organic acid such as acetic acid and citric acid, no residual solvents are present in the generated chitosan particles. Hence, for specific applications where the excess acid condition may not be desirable, such as controlled release drug delivery [23], SCASA process is advantageous.

The XRD analyses (Fig. 10) showed that both processes allowed the generation of repeatable crystal structures but different from commercial chitosan: the intensity ratios I/I_{max} of $2\theta \approx 13^\circ$ peak and $2\theta \approx 20^\circ$ peak were significantly altered during the process. In the literature, these two peaks are assigned to two different structural forms of chitosan: hydrated (13°) and anhydrous (20°) crystals. The peak around $2\theta \approx 30^\circ$, characteristic of residual chitin in commercial chitosan, and the peak around $2\theta \approx 46^\circ$ disappeared. With the SAS process, a halo at $2\theta \approx 23^\circ$ that was attributed to an allomorphic form of chitosan [24] and a well-defined peak at $2\theta \approx 44^\circ$ peak appeared. With the second generation process, two peaks around 27° and 28°, not referenced in previous studies, appeared. Thus, both generation processes significantly modify the crystalline structure of chitosan and make it more amorphous. Although the crystalline structure of chitin has well been studied in the literature, crystallinity of chitosan is still not completely explored, which explains the presence of unassigned peaks.

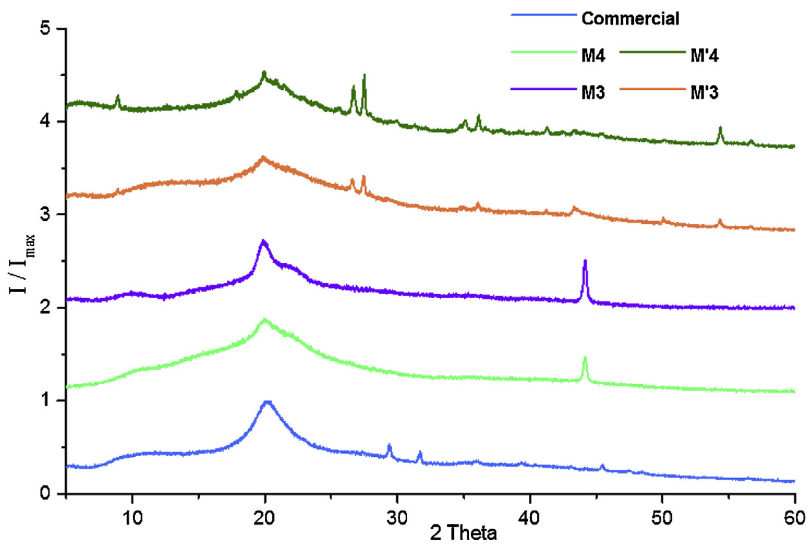

Fig. 10. X-ray diffractograms of the commercial chitosan and chitosan generated by SAS process (M3 and M4) and by SCASA process (M'3 and M'4).

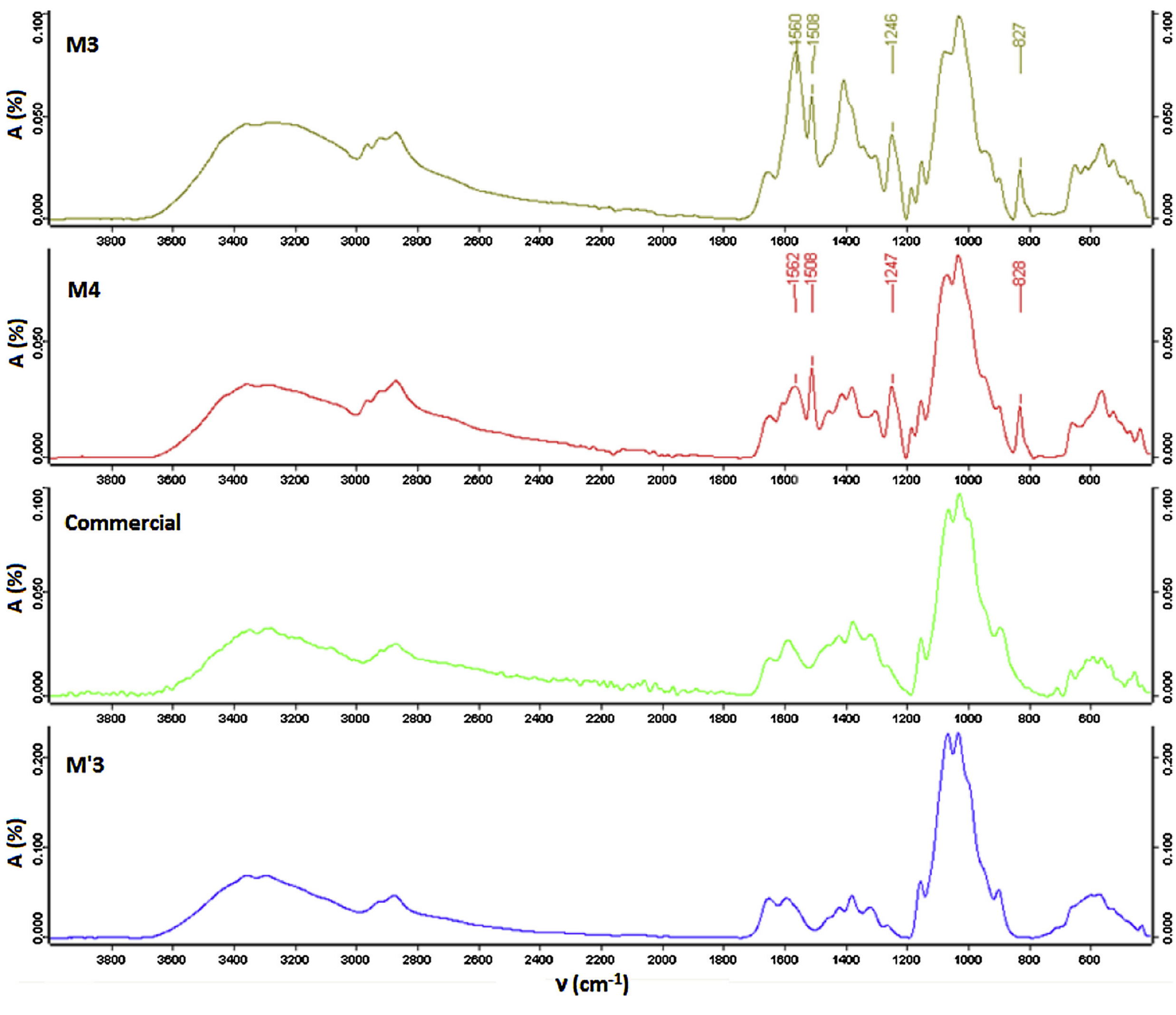

Fig. 11. FT-IR spectra (ATR mode) of the commercial chitosan and chitosan generated by M3, M4 and M'3 tests.

Shen et al. [14] also observed an amorphization of chitosane particles with SAA-HCM process, which was attributed to the sudden supersaturation in the precipitator, which led to a rapid evaporation of the solvent from the droplets and a lower crystallinity of the generated particles. Reverchon and Antonacci [13] attributed the formation of amorphous chitosan particles to a physicochemical modification under the high operating temperatures, possibly related to deacetylation and/or cross-linking of the polymer. In our case, high supersaturation rates are generated during the depressurization through the capillary, which induces the generation of unstable amorphous solid forms.

For all the chitosan particles, the thermal stability analyzed by TGA showed a degradation around 523 K.

The acetylation degree was calculated as previously presented. The DA was $21 \pm 2\%$, $20 \pm 1\%$, $19 \pm 6\%$ and $21 \pm 1\%$ for commercial chitosan, M3, M4 and M'3, respectively (Fig. 11): no significant difference could be assigned to the process; the slight differences may be due to various errors related to the measurement technique. A difference with the DA given by the supplier has been noticed but no rational explanation could be given.

No significant difference could be observed between the IR-spectrometer of M'3 processed by SCASA and commercial chitosan. However, a notable difference could be seen between samples processed by SCASA and by SAS (M3 and M4): several peaks appeared only for SAS process at 825, 1245, 1506 and 1556 cm^{-1}. The peaks at 1245 cm^{-1} and 1506–1556 cm^{-1} refer to C—N and N—H bonds respectively, which means that during the SAS process, a new chemical bond appeared: in fact, according to Nunthanid et al. [25], dissolving chitosan in acetic acid induces the generation of chitosan acetate salts (NH^{3+},$^{-}OOC\text{-}CH_3$) that transform, after drying, to acetyl group present in the (N-acetyl-D-glucosamine) structure of chitin [26]. A similar result was observed by Shen et al. [14].

4. Conclusion

4.1. Supercritical anti-solvent process

In this work, a method for generating chitosan particles by anti-solvent effect using sc-CO_2 has been designed and tested. Nanometer scaled particles were produced with a mean diameter of 378 ± 13 nm and an amorphized structure, which differs from the commercial chitosan. Morphology, aspect and particle arrangement strongly depend on the recovery medium that seems to have an influence through the pH on the phase separation mechanism and the resulting morphology, a porous chitosan network or chitosan particles. Furthermore, particles obtained by these experiments are in majority spherical. In this context, a further study on the stability of the particles in suspension should be performed.

4.2. Sc-CO_2 assisted solubilization and atomization process

A new sc-CO_2 assisted solubilization and atomization process, SCASA, was setup and preliminary experiments were achieved to check its feasibility and repeatability. Three main conclusions can be drawn: firstly, compared to the processes already used to generate chitosan particles, this new process is simple and does not require any organic solvent. Secondly, it is clear that the acidifying strength of the CO_2 allowed the dissolution of chitosan powder. Thirdly, the atomization process generated mostly near-spherical and spherical shaped particles during several experiments, which implied the repeatability of this new process and its robustness, as it is not destabilized by small parameters variations. However, two particle size scales were noticed: nanometric scaled particles with a median diameter of 390 nm and micrometric scaled particles with a mean diameter around 20 μm and made of agglomerated nanoparticles. The presence of individual spherical particles larger than 1 μm should be mentioned but they represented less than 10% of the total measurements. Many of the particles seem hollow-shaped probably due to the CO_2 desorption while particles solidification takes place. Experiments showed that for the used chitosan and configurations, the best results were obtained for CO_2 pressure inside the vessel during spraying of 13–15 MPa with an air flow of 140 $Nm^3\,h^{-1}$ heated to 353 K. A good compromise between the spraying rate and the drying airflow rate should be found. A further step regarding this process will consist in optimizing the process parameters as the solution flow and the flows ratio, drying temperature and the particle-collecting device to finally obtain narrower particle size distribution with a high yield.

In future works, the generated nanoparticles and agglomerates of nanoparticles will be dispersed in a biobased polymer matrix by plastic manufacturing processes to produce nanostructured assemblies.

Acknowledgement

Authors gratefully acknowledge the technical work of Bruno Boyer. This paper is dedicated to the memory of our esteemed colleague Elisabeth Rodier who left us much too early.

References

[1] P. Bordes, E. Pollet, L. Avérous, Nano-biocomposites: biodegradable polyester/nanoclay systems, Progress in Polymer Science 34 (2009) 125–155.
[2] G. Crini, P.M. Badot, E. Guibal, Chitine et chitosane. Du biopolymère à l'application, Presses Universitaires de Franche-Comté, Besançon, 2009.
[3] M.C. Cruz-Romero, T. Murphy, M. Morris, E. Cummins, J.P. Kerry, Antimicrobial activity of chitosan, organic acids and nano-sized solubilisates for potential use in smart antimicrobially-active packaging for potential food applications, Food Control 34 (2013) 393–397.
[4] I. Leceta, P. Guerrero, I. Ibarburu, M.T. Dueñas, K. de la Caba, Characterization and antimicrobial analysis of chitosan-based films, J. Food Engineering 116 (2013) 889–899.
[5] L.Y. Zheng, J.F. Zhu, Study on antimicrobial activity of chitosan with different molecular weights, Carbohydrate Polymers 54 (2003) 527–530.
[6] M.N.V. Ravi Kumar, A review of chitin and chitosan applications, Reactive and Functional Polymers 46 (2000) 1–27.
[7] M. Dash, F. Chiellini, R.M. Ottenbrite, E. Chiellini, Chitosan – a versatile semi-synthetic polymer in biomedical applications, Progress in Polymer Science 36 (2011) 981–1014.
[8] P. He, S.S. Davis, L. Illum, Chitosan microspheres prepared by spray drying, International J. Pharmaceutics 187 (1999) 53–65.
[9] J. Akbuğa, G. Durmaz, Preparation and evaluation of cross-linked chitosan microspheres containing furosemide, International J. Pharmaceutics 111 (1994) 217–222.
[10] H.Q. Mao, K. Roy, V.L. Troung-Le, K.A. Janes, K.Y. Lin, Y. Wang, J.T. August, K.W. Leong, Chitosan–DNA nanoparticles as gene carriers: synthesis, characterization and transfection efficiency, J. Controlled Release 70 (2001) 399–421.
[11] G. Weibel, C.K. Ober, Processing polymers in supercritical CO_2, in: K.H. Buschow, R.W. Cahn, C.M. Flemings, B. Ilschner, E.J. Kramer, S. Mahajan (Eds.), Encyclopedia of Materials: Science and Technology, Elsevier, New York, 2002, pp. 1–8.
[12] J. Fages, H. Lochard, J.-J. Letourneau, M. Sauceau, E. Rodier, Particle generation of pharmaceutical applications using supercritical fluid technology, Powder Technology 141 (2004) 219–226.
[13] E. Reverchon, A. Antonacci, Chitosan microparticles production by supercritical fluid processing, Industrial and Engineering Chemistry Research 45 (2006) 5722–5728.
[14] Y.B. Shen, Z. Du, Q. Wang, Y.X. Guan, S.J. Yao, Preparation of chitosan microparticles with diverse molecular weights using supercritical fluid assisted atomization introduced by hydrodynamic cavitation mixer, Powder Technology 254 (2014) 416–424.
[15] M.X. Weinhold, J.C.M. Sauvageau, N. Keddig, M. Matzke, B. Tartsch, I. Grunwald, C. Kübel, B. Jastorff, J. Thöming, Strategy to improve the characterization of chitosan for sustainable biomedical applications: SAR guided multi-dimensional analysis, Green Chemistry 11 (2009) 498–509.
[16] D.G. Rao, Studies on viscosity–molecular weight relationship of chitosan solutions, J. Food Science and Technology 30 (1993) 66–67.
[17] H.M. Kwaambwa, J.W. Goodwin, R.W. Hughes, P.A. Reynolds, Viscosity, molecular weight and concentration relationships at 298 K of low molecular weight

cis-polyisoprene in a good solvent, Colloids and surfaces A: Physicochemical and Engineering Aspects 294 (2007) 14–19.
[18] L. Diamond, N. Akinfiev, Solubility of CO_2 in water from -1.5 to $100\,^{\circ}C$ and from 0.1 to 100 MPa: evaluation of literature data and thermodynamic modelling, Fluid Phase Equilibria 208 (2003) 265–290.
[19] C. Peng, J.P. Crawshawa, G.C. Maitlanda, J.P. Martin Truslera, D. Vega-Mazab, The pH of CO_2-saturated water at temperatures between 308 K and 423 K at pressures up to 15 MPa, J. Supercritical Fluids 82 (2013) 129–137.
[20] A.J. Read, The first ionization constant of carbonic acid from 25 to $250\,^{\circ}C$ and to 2000 bar, J. Solution Chemistry 4 (1) (1975) 53–70.
[21] M. Kasaai, A review of several reported procedures to determine the degree of N-acetylation for chitin and chitosan using infrared spectroscopy, Carbohydrate Polymers 71 (2008) 497–508.
[22] M. Mulder, Basic Principles of Membrane Technology, 2nd ed., Kluwer Academic Publishers, Dordrecht/Boston/London, 1997.
[23] S. Puttipipatkhachorn, J. Nunthanid, K. Yamamoto, G.E. Peck, Drug physical state and drug–polymer interaction on drug release from chitosan matrix films, J. Controlled Release 75 (2001) 143–153.
[24] M. Jaworska, K. Sakurai, P. Gaudon, E. Guibal, Influence of chitosan characteristics on polymer properties. I: crystallographic properties, Polymer International 52 (2003) 198–205.
[25] J. Nunthanid, A. Laungtana-Anan, P. Sriamornsak, S. Limmatvapirat, S. Puttipipatkhachorn, L.Y. Lim, E. Khor, Characterization of chitosan acetate as a binder for sustained release tablets, J. Controlled Release 99 (2004) 15–26.
[26] M. Rinaudo, Chitin and chitosan: properties and applications, Progress in Polymer Science 31 (2006) 603–632.